Green synthesis and biological evaluation of novel 5-fluorouracil derivatives as potent anticancer agents

Farhat Jubeen, Aisha Liaqat, Misbah Sultan, Sania Zafar Iqbal, Imran Sajid and Farooq Sher

Original citation & hyperlink:
Jubeen, Farhat, et al. "Green synthesis and biological evaluation of novel 5-fluorouracil derivatives as potent anticancer agents." *Saudi Pharmaceutical Journal*, Vol 27, Issue 8, pp. 1164-1173 (2019).
https://dx.doi.org/10.1016/j.jsps.2019.09.013

ISSN 1319-0164

Publisher: Elsevier

Saudi Pharmaceutical Journal 27 (2019) 1164–1173

Contents lists available at ScienceDirect

Saudi Pharmaceutical Journal

journal homepage: www.sciencedirect.com

Original article

Green synthesis and biological evaluation of novel 5-fluorouracil derivatives as potent anticancer agents

Farhat Jubeen [b], Aisha Liaqat [b], Misbah Sultan [c], Sania Zafar Iqbal [b], Imran Sajid [c], Farooq Sher [a,d,*]

[a] Department of Chemical and Environmental Engineering, University of Nottingham, University Park, Nottingham NG7 2RD, UK
[b] Department of Chemistry, Government College Women University, Faisalabad 38000, Pakistan
[c] Department of Chemistry, University of the Punjab, Lahore 54590, Pakistan
[d] School of Mechanical, Aerospace and Automotive Engineering, Coventry University, Coventry CV1 5FB, UK

ARTICLE INFO

Article history:
Received 12 July 2019
Accepted 28 September 2019
Available online 31 October 2019

Keywords:
5-Fluorouracil
Co-crystals
Green synthesis
Supramolecular interactions
Grinding and solution method

ABSTRACT

This study reports the formation of 5-FU co-crystals with four different pharmacologically safe co-formers; Urea, Thiourea, Acetanilide and Aspirin using methanol as a solvent. Two fabrication schemes were followed i.e., solid-state grinding protocol, in which API and co-formers were mixed through vigorous grinding while in the other method separate solutions of both the components were made and mixed together. The adopted approaches offer easy fabrication protocols, no temperature maintenance requirements, no need of expensive solvents, hardly available apparatus, isolation and purification of the desired products. In addition, there is no byproducts formation, In fact, a phenomenon embracing the requirements of green synthesis. Through FTIR analysis; for API the N—H absorption frequency was recorded at 3409.02 cm^{-1} and that of —C=O was observed at 1647.77 cm^{-1}. These characteristics peaks of 5-FU were significantly shifted and recorded at 3499.40 cm^{-1} and 1649.62 cm^{-1} for 5-FU-Ac (3B) and 3496.39 cm^{-1} and 1659.30 cm^{-1} for 5-FU-As (4B) co-crystals for N—H and —C=O groups respectively. The structural differences between API and co-crystals were further confirmed through PXRD analysis. The characteristic peak of 5-FU at 2θ = 28.79918° was significantly shifted in the graphs of co-crystals not only in position but also with respect to intensity and FWHM values. In addition, new peaks were also recorded in all the spectra of co-formers confirming the structural differences between API and co-formers. In addition, percent growth inhibition was also observed by all the co-crystals through MTT assay against HCT 116 colorectal cell lines *in vitro*. At four different concentrations; 25, 50, 100 and 200 μg/mL, slightly different trends of the effectiveness of API and co-crystals were observed. However; among all the co-crystal forms, 5-FU-thiourea co-crystals obtained through solution method (2B) proved to be the most effective growth inhibitor at all the four above mentioned concentrations.

1. Introduction

Cancer is abnormal and uncontrolled growth and multiplication of cells. It is the second major cause of casualties each year. A number of treatment strategies and medicines have been explored and evaluated. However, none of them is producing satisfactory outcomes. Almost all the chemotherapy medicines have associated drawbacks, and studies are being carried out to minimize their side effects (Zhang, 2018). Chemical derivatization of an active pharmaceutical drug to mask its undesirable effects and to deliver unaltered at the site of action is a modern and fascinating approach to optimize the desired effects. The exploration of essential functionalities of heterocyclic compounds in medicinal field is a widely studied domain (Zha, 2019). Certain structural features of compounds are responsible for their diverse activities (Zhao, 2018). Nitrogen containing heterocyclic compositions are vital components of many natural compounds e.g., antibiotics, vitamins and nucleic acids (Jubeen, 2018; Rakesh, 2017; Moku, 2019; Wang, 2018). 5-fluorouracil (5-FU), antimetabolite of pyrimidine, a mainstream anticancer drug has been studied widely since its discovery in 1957 (Jubeen, 2018; Carrillo, 2015). The derivative of enone functional group in 5-FU molecule is similar to many natural and synthetic α,β-unsaturated carbonyl based compounds like chalcones, curcumin etc. responsible for antitumor activities having strong antiproliferative potential (Qin, 2016, 2017; Zha, 2017). 5-FU administration, either intravenous, oral or topical has

* Corresponding author at: School of Mechanical, Aerospace and Automotive Engineering, Faculty of Engineering, Environment and Computing, Coventry University, Coventry CV1 2JH, UK.
E-mail address: Farooq.Sher@coventry.ac.uk (F. Sher).

https://doi.org/10.1016/j.jsps.2019.09.013
1319-0164/

associated drawbacks of short plasma half-life, non-targeted cytotoxicity and other health related issues e.g., alopecia, vomiting, diarrhoea (Radwan and Alanazi, 2014; Miura, 2010). For the reduction of side effects and short comes associated with 5-FU chemotherapy, 5-FU and its derivatives are under keen consideration.

Many derivatives of 5-FU have been formulated and studied following a number of different approaches. Derivatization with macromolecules e.g., carbohydrates or lipid moieties were fabricated for crossing the membrane barriers and improving the solubility related drawbacks (Zhang, 2018; Petaccia, 2016; Köksal Karayildirim, 2018). Considering the fact of pH difference in different organs and tissues, a variety of pH sensitive prodrugs of 5-FU has been designed for its targeted action (Ofonime Udofot, 2015). Further working on target selectivity, 5-FU modification has also been done with various DNA binders, a phenomenon termed as DNA intercalation e.g., binding of DNA binder drugs to the N^1 or N^3 or at both positions simultaneously (Zhou, 2013). Further heading towards improving drug potency of 5-FU chemotherapy with no or minimum side effects, a variety of 5-FU loaded nanoparticles have been designed for improving surface to volume ratio resulting in maximum drug entrapment and easy travelling to targeted tissues (Tummala et al., 2015; Subudhi, 2015; Dong, 2019). Furthermore, co-crystallisation of 5-FU (active pharmaceutical ingredient) with co-formers is an emerging and novel phenomenon for reversible inactivation of 5-FU (Stoler and Warner, 2015).

Co-crystallisation of 5-FU is feasible and advantageous as it has both hydrogen bond donor and acceptor groups (Nadzri, 2016). The central focus lying behind increasing interest in this domain is easy fabrication requirements i.e., designing methodologies of co-crystals are comparatively easy, no requirement of costly and scarcely available instruments, feasible at room temperature, solvents are required in a very low amount or sometimes solvent free methodologies can also be followed (Douroumis et al., 2017; Karimi-Jafari, 2018; Likhitha, 2019). Likewise, this phenomenon is also free from side products formation or isolation and purification. As this is a very new and innovative phenomenon, there is not much work found in the literature.

Successful co-crystals of 5-FU were reported with some aromatic compounds, benzoic acid derivatives and heterocyclic compounds (Delori et al., 2013; Mohana et al., 2017; Dai, 2016). However, in none of the published studies, the safety of co-formers regarding antimetabolites formation in the body is mentioned. Further, there is no evidence of any co-crystal reported in the literature for their anticancer activity (MTT assay). Most of the studies are mainly focused on the structure elucidation from the point of view of the development of supra-molecular interactions. Reported literature is lacking of the data regarding biological activity of the synthesised co-crystals (Nadzri, 2016; Dai, 2016).

This research explains the fabrication of co-crystals of 5-FU with four different compounds i.e., urea, thiourea, acetanilide and aspirin. All the selected co-formers have hydrogen bond donor or acceptor groups or both. In addition to the feasibility of supra-molecular interactions, all of these four molecules manifest much significance regarding their biological activities from a pharmaceutical point of view. Further, their metabolism in the body does not result in toxic metabolites so, this selection of co-formers is not only safe for *in-vivo* administration but can also be helpful in the improvement of 5-FU pharmacological properties (Langley and Rothwell, 2012; Li, 2017; Rakesh, 2017). The major elements in all the selected co-formers like F, S, O, N and H are among the top ten elements in approved drugs (Fang, 2019). Co-crystals of 5-FU are prepared by following the solid-state grinding method and solution method, with the use of methanol as a solvent. Methanol was selected considering the non-reactivity of alcohols, as the OH group in alcohols as leaving group cannot be easily replaced. In none of the protocols hazardous chemicals were required. Further the required apparatus was economical and easily available. No by-products were formed. Co-crystals grew on ambient temperature and pressure (Ahmed, 2016). In short, both the fabrication methodologies followed in this study clearly manifest and fulfil the conditions of green synthesis (Ansari, 2019). Formation of supra-molecular interactions was evaluated through FTIR and structural differences between API and co-crystals were evaluated through powdered XRD analysis of fabricated co-crystals. Comparative study of API and co-crystals from the FTIR spectra proved the development of hydrogen bonding interactions and the shift of characteristic 5-FU peak in PXRD graphs of co-crystals proved the structural differences of 5-FU and co-formers. Furthermore, *in vitro* anticancer assays of the designed crystals are also performed for their biological evaluation. All the co-crystals proved to be effective for the growth inhibition of *actinomycetes* more or less than the main API. Four different concentrations of *actinomycetes* were applied to variate the number of viable cells and consequently the outcomes of synthesised co-crystals at different concentrations were evaluated (Suthindhiran and Kannabiran, 2009). The novelty of this study over others is its analysis and identification approach for the selection of the more prolific method for co-crystals fabrication from two available, under standard conditions. Apart from this, the two of the synthesised co-crystals are novel, has not been synthesised previously including acetanilide and aspirin's co-crystals with 5-FU. In literature, the co-crystals formation was mostly confirmed through XRD analyses, but this research provides strong chemical shreds of evidence of co-crystals formation by the help FTIR analyses in addition to XRD analyses.

2. Experimental

2.1. Chemicals

5-FU was provided by (Sigma-Aldrich, 99%), other chemicals used in the study are urea (Applichem Biochemica Chemical synthesis services, 98%), thiourea (Merck KGaA, 98%), acetanilide (UNI CHEM chemical reagents, 99%) and aspirin (AnalaR chemicals Ltd. Poole England). Methanol (Merck KGaA, 99.5% purity) was used to facilitate crystallisation and dissolution. All the chemicals were used without further purification. Co-crystals of 5-FU are designed with urea, thiourea, acetanilide and aspirin following solid-state grinding method (Nadzri, 2016; Sonawane, 2014) and solution method with little modification in the synthesis protocol of (Moisescu-Goia et al., 2017).

2.2. Synthesis of co-crystals

2.2.1. Solid state grinding method

The calculated amounts, 4.4 mM, of API (0.572 g) and co-former (acetanilide, 0.56 g; aspirin, 0.792 g; urea, 0.24 g and thiourea, 0.32 g) were weighed and mixed vigorously for about 30 minutes with the help of motor and pestle, then the ground mass was dissolved in methanol to form a solution (Sonawane, 2014). A clear solution was obtained without heating in the case of acetanilide co-formers while in all the other three cases heating was done to get a clear solution. After the clear solution formation vials were cooled at room temperature, covered with aluminium foil and placed for crystal growth. Colourless crystals were obtained in all the four cases

2.2.2. Non- grinding solution method

The weighed amounts of API and co-formers as mentioned above were taken in 1:1 ratio, dissolved in methanol in separate

vials, after that each vial was heated at water bath to get the clear solution of both the members. Then the hot solutions of API and each co former were transferred in a single vial and warmed at about 90–100 °C for about 3 minutes, then these solutions were cooled at room temperature, covered with aluminium foil with 1 hole in it and placed in a dark cupboard for evaporation and crystal growth (Moisescu-Goia et al., 2017; Yan, 2009).

2.3. Characterisation

2.3.1. FTIR and PXRD

In order to study the changes in vibrational modes of functional groups responsible for hydrogen bonding, FTIR analysis was performed. Spectra of co-crystals were compared to the spectrum of 5-FU alone and shifting of —N—H groups and -C=O from normal peaks were evaluated to study the development of non-covalent interactions for co-crystals formation (Moisescu-Goia et al., 2017). The Co-crystals were further evaluated through PXRD (Dai, 2016; Moisescu-Goia et al., 2017; Li et al., 2014). PXRD phenomenon is based on constructive interference between monochromatic X-rays and crystalline samples. X-rays were generated by cathode ray tube, filtered to get monochromatic rays, assembled to concentrate and then directed towards the sample. MTT assay was performed to bio-evaluate the as prepared co-crystals (Petaccia, 2016; Fang, 2015).

2.3.2. In vitro MTT antitumor bioassay

HCT 116 human colorectal cancer cell line ATCC®CCL-247™ [(catalogue no: 91091005-1VL) Sigma Aldrich] was used. Cells were cultured as a monolayer in T-75 flasks Costar, followed by subculturing twice a week at 37 °C in 5% CO_2 and 100% relative humidity supplied incubator and managed at low passage number 5 to 20. HCT 116 was cultured in McCoy's 5A medium Gibco Glasgow, supplemented with 10% fetal bovine serum FBS (Qin, 2015); Gibco, Glasgow, UK and 1% antibiotics (streptomycin, penicillin).

Adherent cells at a logarithmic growth phase were washed with 2 mL of PBS (phosphate buffered saline). Afterwards detached by addition of 0.5 mL of 1X trypsin and incubated for 2–5 min at 37 °C in the incubator. 100 μL complete growth media was added per well in 96-well flat-bottom microplates. Then cells were counted for desired densities by staining with trypan blue and counted with a hemacytometer. Each well was inoculated at densities of 1,000–100,000 cells per well (Fang, 2015). Afterward cells were treated with different concentrations of actinomycete extracts such as 12 , 25, 50 and 100 mg/mL. Actinomycetes, gram-positive bacteria, have been recognized as sources of several secondary metabolites, antibiotics and bioactive compounds that affect microbial growth. The experiment was performed in triplicates to avoid any error. Background control wells containing the same volume of complete culture medium was included in each experiment along with a positive control containing Triton X-100 and negative controls as well. The plate was incubated at 37 °C for 24 h in CO_2 supplied humidified incubator (Vichai and Kirtikara, 2006).

After 24 hours, 10 μL of 3-(4, 5-dimethyl thiazol-2-yl)-2, 5-diphenyl tetrazolium bromide (MTT) was directly added in the culture media of each well. The plate was incubated for 4 hours at 37 °C in 5% CO_2 incubator. After incubation plate was removed from the incubator and gently culture media was removed without disturbing cells monolayer. Subsequently, 100 μL of DMSO (dimethyl sulfoxide) was added in each well and plate was shaken to solubilize formazan (Patel, 2009). Absorbance was recorded spectrophotometrically at 570 nm. The inhibitory rate was calculated and plot graphs against all actinomycetes extract to evaluate their anticancer activities. Subsequently, IC_{50} was calculated for each extract. The growth inhibition rate was calculated by the following equation:

$$\%\text{Mortality} = \frac{\text{O.D(control well)} - \text{O.D(treated well)}}{\text{O.D(control well)}} \times 100$$

3. Results and discussion

The type and the extent to which the interactions were developed between API and co-formers and their biological effectiveness were evaluated through comparison of results of as synthesised co-crystal with API.

3.1. Comparative analysis of the development of supramolecular interactions by FTIR spectroscopy

Spectra of all the synthesised eight co-crystals were studied in comparison to the API. The absorption frequencies of the main peaks of interest involved in hydrogen bonding interactions are arranged in Table 1. The main peaks of interest are those arising from the absorption of N—H (hydrogen bond donor) and C=O (Hydrogen bond acceptor) groups in all the spectra. In the IR spectrum of 5-FU, a blunt peak at 3409.02 cm^{-1} could be attributed to υ (N—H) while a broad pointed band of high intensity at 1647.77 cm^{-1} could be attributable to absorption of C=O groups (Abdelghani, 2017).

3.1.1. 5-FU-U (1A and 1B)

A strong absorption peak at 3438.20 cm^{-1} and a low absorption peak at 3556.93 cm^{-1} showing hypochromic shift as compared to 5-FU in the spectrum of co-crystals of 5-FU-U obtained through grinding method were found. The peak at 3438.20 cm^{-1} in the co-crystal spectrum had shown a regular hypochromic shift in comparison to API (Fig. 5). While the other peak with a huge difference in absorption frequency and peak shape and size in comparison to 5-FU may be arisen due to the N—H groups of urea. In the other spectrum of 5-FU-U co-crystals obtained through solution method, a less pointed peak of medium intensity arose at 3437.62 cm^{-1} following the exact blue shift in absorption frequency of N—H groups of co-crystals as described in the published literature on the same phenomenon (Nadzri, 2016).

In the co-crystals of 5-FU-U, synthesised through grinding method Fig. 5 (1A), strong absorption peaks at 1633.23 cm^{-1} and 1562.88 cm^{-1} were representative of C=O absorption indicating a bathochromic shift. While in solution method, Fig. 5 (1B), 1614.94 cm^{-1} and 1559.95 cm^{-1}, could be the result of C=O absorptions. In short, for 5-FU-U co-crystals, strong red shifts for both the spectra of co-crystals were observed for carbonyl group absorptions as compared to API indicating the stretching of C=O bond and development of single bond character due to extensive involvement of O-atoms in wander walls interactions as shown

Table 1
Comparison of absorption peaks of groups responsible for supramolecular interactions.

Sample ID	υ (C=O) cm^{-1}	υ (N—H) str cm^{-1}
5-FU	1647.77	3409.02
5-FU-U (1A)	1633.23	3556.93, 3438.20
5-FU-U (1B)	1614.94	3437.62
5-FU-Th (2A)	1610.38	3599.96, 3493.97, 3376.24
5-FU-Th (2B)	1621.81	3568.20, 3388.06
5-FU-Ac (3A)	1663.09	3538.09, 3472.57
5-FU-Ac (3B)	1649.62	3499.40, 3555.67
5-FU-As (4A)	1678.63	3565.19, 3492.82
5-FU-As (4B)	1659.30	3496.39, 3560.13

in Fig. 1. Enhanced red shifts for -C=O groups absorptions in the co-crystal spectrum of solution method were indicative of increased stretching of -C=O bond due to increased supramolecular interactions developing the single bond character and reducing the absorption frequency in turn. This suggests the more suitability of solution method than grinding method for co-crystal fabrication in this case.

3.1.2. 5-FU-Th (2A and 2B)

In the case of 5-FU-Th co-crystal; from all the three peaks for N—H absorptions in co-crystal spectrum of grinding method, 3599.96, 3493.97, 3376.24 cm^{-1}, and two proposed peaks, 3568.20, 3388.06 cm^{-1} in the spectrum of solution method (Table 1), 3493.97 and 3568.20 cm^{-1} attributable to N—H groups of 5-FU were indicating the strong blue shift as compared to API according to the general trend possibly due to the replacement of stronger interactions in the co-formers and API alone, with the weaker interactions while forming co-crystals (Fig. 2) resulting in the less stretching of N—H bond which consequently appeared as higher frequency peaks in the spectra. The extra peaks might be as a result of N—H absorptions of co-formers.

In the case of 5-FU-Th co-crystals; peak at 1610.38 cm^{-1} in the spectrum of co-crystals of grinding method Fig. 6(2A) could be due to carbonyl group absorption of 5-FU, and red shift could be easily justified as the development of single bond character due to Wander Walls interactions, while the hypochromically shifted peak in the spectrum of solution method at 1621.81cm^{-1} is either due to C=O groups or it could also be due to the absorptions of N—H scissoring vibrations as shown in Fig. 6 (2A). More absorption frequency of the N—H groups of co-crystals obtained through solution method Fig. 6 (2B) is in support of greater feasibility of solution method for 5-FU-Th co-crystals fabrication than grinding method.

3.1.3. 5-FU-Ac (3A and 3B)

In the spectrum of 5-FU-Ac co-crystals obtained through grinding method, Fig. 7 (3A), blue shift was observed for the ν (N—H) absorptions in co-crystals i.e., peaks were found at 3538.09 and 3472.57 cm^{-1} in comparison to the spectrum of API. This hypochromic effect is indicative of the strengthening of N—H bond due to replacement of already present interactions with the new

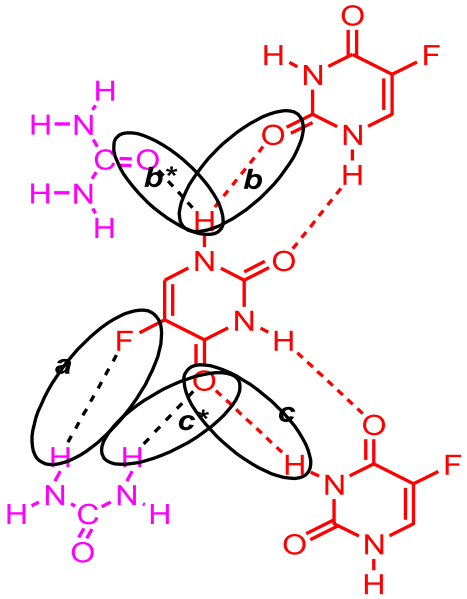

Fig. 1. Proposed interactions between 5-FU-U co-crystals.

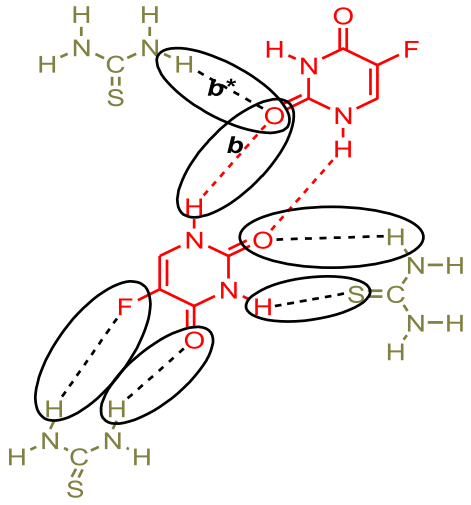

Fig. 2. Proposed interactions between 5-FU-Th co-crystals

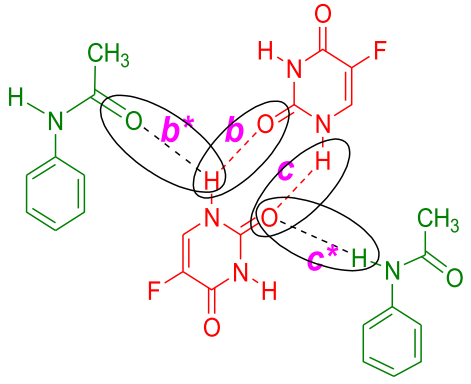

Fig. 3. Proposed interactions between 5-FU-Ac co-crystals.

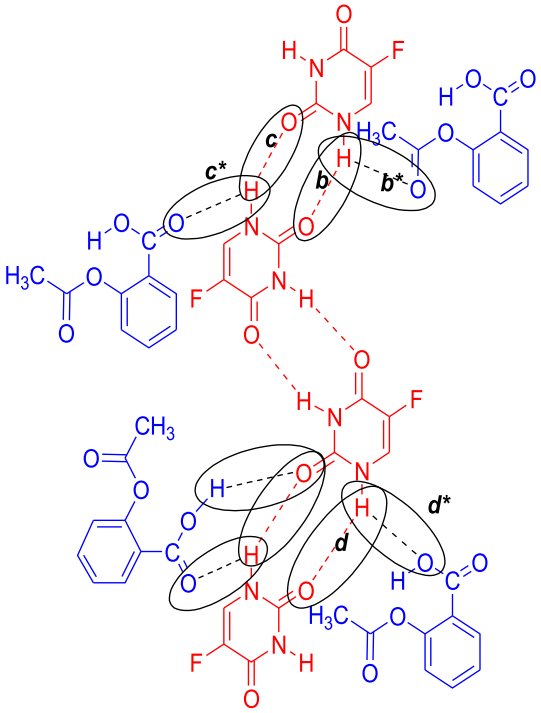

Fig. 4. Proposed interactions between 5-FU-As co-crystals.

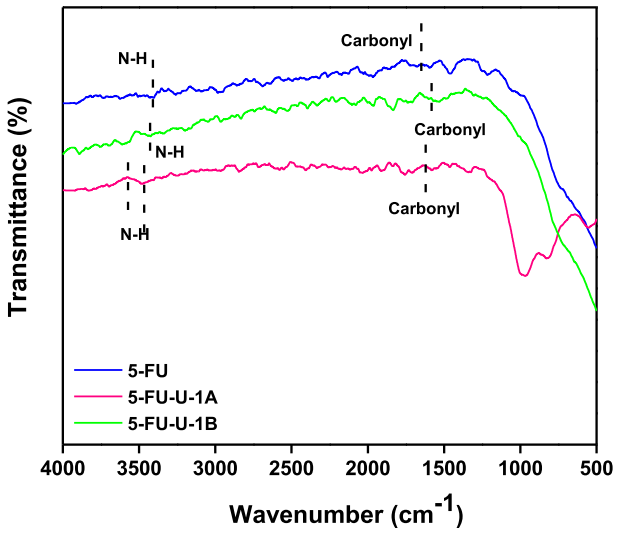

Fig. 5. Comparative FTIR spectra of 5-FU-U co-crystals fabricated by grinding (A) and solution (B) method.

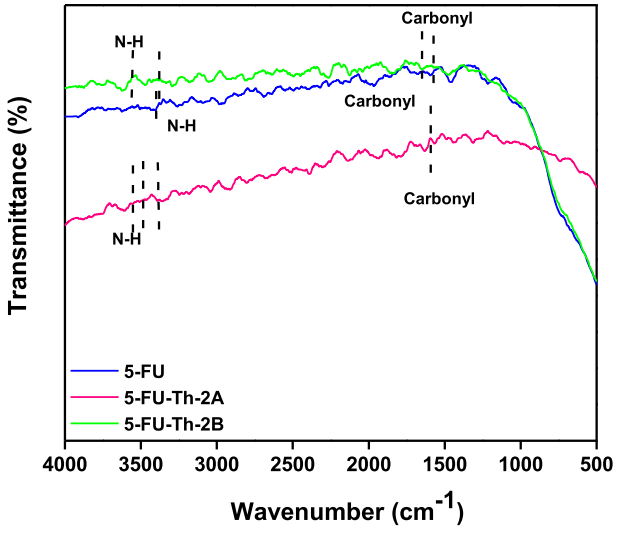

Fig. 6. Comparative FTIR spectra of 5-FU-Th co-crystals fabricated by grinding (A) and solution (B) method.

interactions involving co-formers as shown in Fig. 3. Intermolecular hydrogen bonding interactions of 5-FU (***b***) were replaced by ***b**** interactions making the N—H bond more stronger and shifting the absorption towards shorter wavelength i.e., at 3538.09 and 3472.57 cm^{-1} (Moisescu-Goia et al., 2017). The reason behind this may be the attachment of acetanilide C to electron donating methyl group which consequently enhanced the N—H bond strength as compared to the C of 5-FU which was attached to two inductively electron withdrawing N atoms.

Two blunt peaks were observed in the spectrum of 5-FU-Ac co-crystals obtained through solution method Fig. 7 (3B) which could be attributed to N—H absorption i.e., at 3555.67 cm^{-1} and 3499.40 cm^{1}. Both peaks followed a hypochromic shift as compared to API. That significant change in absorption frequency was indicative of major changes in the N—H interactions as explained for the co-crystals obtained through the grinding method and illustrated in Fig. 3.

Carbonyl groups in the co-crystal spectrum were found to exhibit the most intense or second most intense peaks in the spectra. There was significant hypochromic shift in the frequency of carbonyl groups of co-crystals obtained through grinding method than that of 5-FU, indicating the alteration of hydrogen bonding interactions of carbonyl groups in 5-FU as shown in Fig. 3, there was low possibility of b* as compared to c* due to the steric hindrance of methyl group in b*. The absorption frequency of carbonyl groups in the spectrum of the solution method was also slightly shifted in 5-FU and co-crystals. More absorption frequency of N—H groups was indicative of more strengthening of this bond following solution method as compared to grinding method for co-crystal fabrication. Lower absorption frequency of carbonyl groups in the solution method was indicative that the development of single bond character was more as a result of its involvement in supramolecular interactions. After the discussion, the observations are leading towards the development of 5-FU-Acetanilide co-crystals, solution methodology is claimed to be more effective.

3.1.4. 5-FU-As (4A and 4B)

Hypochromic shift in absorption frequencies of N—H in both the spectra of 5-FU-As co-crystals was indicative of strengthening of this bond possibly owing to replacement of already present interactions with weaker interactions i.e., replacement of 5-FU with aspirin molecules in the neighbor resulting in more strained and less strong interactions which could be attributed to the bigger molecular size of aspirin as compared to 5-FU as indicated in Fig. 4, interactions *b* could be replaced by *b** and *d* could be replaced by *d**.

In the spectrum, 5-FU-As, of co-crystals through grinding method, absorption due to carbonyl groups of 5-FU are not visible in the spectrum of co-crystals possibly in consequence of the involvement of these carbonyl groups in supramolecular interactions and lowering of double bond character due to increased stretching and single bond character of carbonyl groups of 5-FU. This evidence is further supported by a strong band in 1050-1250 cm^{-1} region responsible for C-O absorption (1242.00 cm^{-1} and 1179.10 cm^{-1}). While the absorption frequency of carbonyl group in the co-crystal spectrum of solution method Fig. 8 (4B) was indicative of strong blue shift as compared to that of 5-FU. It indicates the strengthening of the double bond character of C=O group possibly due to the weakening of hydrogen bonding interactions of O atom as shown in Fig. 4 through the interactions d which could be replaced by d* and c could be replaced by c*. N—H absorption peaks were almost at same positions and were of same frequency, so there was no significant change in those interactions in the co-crystals obtained through both the methods. The carbonyl absorption frequency was lower for the co-crystals of solution method as compared to that of grinding method Fig. 8 (4A), indicating the development of single bond character resulting due to the involvement of oxygen of carbonyl group in hydrogen bonding interactions. In short, for the co-crystal synthesis of 5-FU-Aspirin, solution method might be more favourable than the grinding method.

The hypochromic shift in absorption frequencies of N—H groups (Dai, 2016) in the FTIR spectras of Figs. 5–8 are indicative of strengthening of this bond possibly owing to a replacement of already present interactions with weaker interactions resulting in more strained and less strong interactions which could be attributed to the interference of different molecules (co-formers). These prominent blue shifts in ν(N—H) str cm^{-1} absorption frequencies in comparison to 5-FU were in exact accordance with the shifts reported by Nadzri and co-workers (Nadzri, 2016). Considering the 5-FU-acetanilide and 5-FU-aspirin, lower absorption frequency of carbonyl groups in the solution method was indicative that the development of single bond character was more as a result of its involvement in supramolecular interactions. In the same way, the absorption frequencies of N—H and C=O groups indicated that

for the synthesis of 5-FU-Urea and 5-FU-Th, solution method might be more favourable than the grinding method.

3.2. Structural differentiation of API and co-crystals by PXRD

After a clear indication of more favorability of the solution method, the co-crystals formation was further confirmed through powdered XRD. The shifts in the peaks of 5-FU are significant in all the co-crystal forms with respect to both the shapes of the peaks and the intensity of the peaks. These shifts are clearly indicative of the change in the structural characteristics of 5-FU due to the change in intermolecular interactions with different co-formers (Moisescu-Goia et al., 2017). From the stacked graph of API and co-crystals Fig. 13, the most intense characteristic peak of 5-FU recorded at 2θ = 28.80 which is exactly equal to the value reported in the study of Goia et al. (Moisescu-Goia et al., 2017). This characteristic value of 5-FU seemed to be significantly shifted in the graphs of all the co-crystals. For 5-FU-U (1B) co-crystals (Fig. 13), the most intense peak is recorded at 2θ = 28.19. The intensity of this peak is much lower than that recorded for API's characteristic peak manifesting the decreased preferred orientation. It means that the arrangement of molecules in a specific orientation is not appreciable. The crystal size is also not significantly bigger than the API and can be attributed to the smaller size of the urea molecule. The obtained results proved the less crystallinity of the synthesised co-crystals.

For 5-FU-Th (Fig. 13 2B) the most intense peak is recorded at 2θ=27.97. The maximum value of intensity is recorded as compared to API and all the co-crystal forms manifesting the enhanced crystal packing in a specific orientation. The crystal size is also quite bigger as compared to all the other cases except 5-FU acetanilide possibly due to the smaller molecule of thiourea that acetanilide. Now if we talk about 5-FU- Ac co-crystals (Fig. 13 3B), the most intense peak found at 2θ = 29.10. This peak is different from that found in the graph of API not only in the position but also in its intensity and FWHM values are varied significantly, than the values recorded for 5-FU (Table 3). The increase in the intensity value is indicative of the increase in the preferred orientation because of enhanced crystallinity. The much smaller value of the FWHM value is indicative of the significant greater size of co-crystals than API (Table 3) proving the presence of both the constituents in the synthesised co-crystals. The obtained results prove the good crystallinity and structural differences of co-crystals of 5-FU-Ac as compared to API obtained through solution method.

The most intense peak of 5-FU-As (Fig. 13 4B) is recorded at 2θ = 28.74. Although the difference in 2θ value is smaller between API and co-crystals, however, the intensity of this peak is much higher than that of API proving the increased crystallinity of co-crystals. The crystal size is quite smaller in this case. From the above mentioned facts, the least difference in 2θ values is observed between 5-FU and aspirin. However, the difference in the peak shapes, intensity and FWHM values are very much different in both the API and 5-FU-As co-crystals.

For further clarity, the difference in intensities, 2θ values and FWHM values of most prominent peaks are arranged in the tabular form (Table 3). In addition to the shift of 5-FU characteristic peaks, there are many new peaks observed in the graphs of co-crystals and many of the other peaks found in the graph of 5-FU are missing in the graphs of co-crystals. The significant differences in the values and appearance of new peaks are indicative of the variations in the already present 5-FU system manifesting the alterations in already present supramolecular interactions due to the incorporation of different co-formers forming co-crystals. Crystallite size of all the co-crystal and API is calculated from Scherrer equation (Table 3) (Li et al., 2014). Although the size difference between urea and thiourea is not significant, however the crystallite size of 5-FU-Th is almost double than that calculated for 5-FU-U co-crystals. This significant difference might be attributed to the most compact and strong hydrogen bonding interactions in 5-FU urea co-crystals than that in the 5-FU-Th co-crystals.

This effect arises due to the involvement of all the groups of urea in hydrogen bonding interactions while in thiourea, sulphur in place of oxygen is not a good candidate for the development of hydrogen bonding interactions leading to loose crystal packing. This is also confirmed by FTIR results and from MTT assay the more anticancer potential of 5-FU thiourea co-crystals as compared to 5-FU-U co-crystals also confirms the loose packing and easy release of API. In short, the crystal size of all the co-crystals is also indicative of the successful formation of strong hydrogen bonding interactions as all the co-crystals are significantly bigger in size than the 5-FU alone manifesting the incorporation of co-formers with API, forming supramolecular synthons.

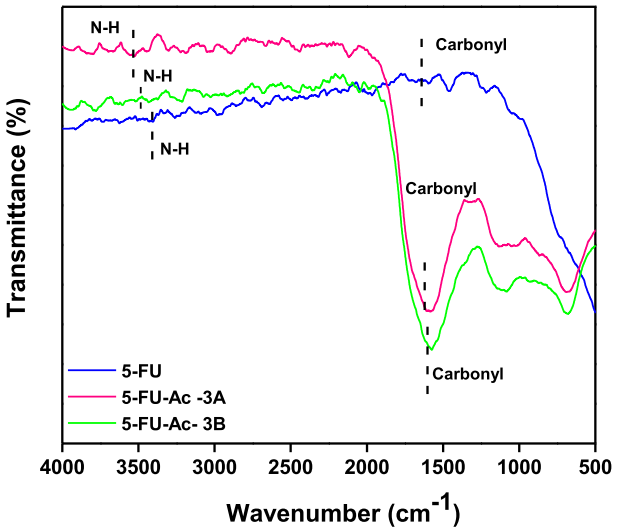

Fig. 7. Comparative FTIR spectra of 5-FU-Ac co-crystals fabricated by grinding (A) and solution (B) method.

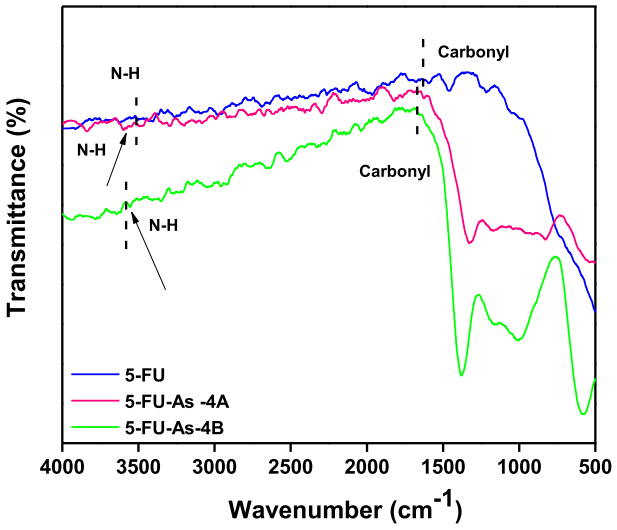

Fig. 8. Comparative FTIR spectra of 5-FU-As co-crystals fabricated by grinding (A) and solution (B) method.

3.3. Evaluation of in vitro anticancer potential of co-crystals

Figs. 9–12 explain the comparative study of the rate of % growth inhibition in relation to changing the concentration of *Actinomycetes*, of the fabricated co-crystals via grinding (A) and solution method (B). All the co-crystals proved to be effective for growth inhibition to a variable extent against HCT 116 colorectal cell lines *in vitro*. 5-FU manifested a gradual increase in percent growth inhibition with the increase in the concentration of *actinomycetes* Table 2 (Fang, 2015). Its maximum growth inhibition potential is 64.48% at 200 μg/mL concentration. This trend of increasing growth inhibition with increasing concentration of *actinomycetes* is very much rational i.e., as the concentration of microorganism's extract is increased, the drugs will have more targets to act upon and consequently, the numerical values of inhibition will also increase.

It is obvious that in all the cases percentage growth inhibition is directly related to the *actinomycetes* concentration except for 5-FU-urea co-crystals obtained through grinding method (1A). For 1A co-crystals this trend is diverted from the observed trend only at 200 μg/mL i.e., for 1A co-crystals 100 μg/mL proved to be the concentration responsible for highest growth inhibition of 40.255% while in all the rest of the cases in addition to API alone 200 μg/mL is the concentration responsible for maximum growth inhibition as shown in Fig. 9. On the other hand, 1B co-crystals of 5-FU-U has a maximum anticancer potential of 45.7195% at 200 μg/mL. The observed difference in the anticancer potential of API alone and co-crystals of 5-FU-U is attributed to the free and bounded conditions of 5-FU (Fig. 9).

From Table 2 it is clearly observed that the co-crystals of 5-FU-Th obtained through solution method (Fig. 10 (2B)) are much more effective in the percent growth inhibition than that obtained through grinding method Fig. 10 (2A). At all the four concentrations the anticancer potential of 2B co-crystals are comparable to that of 5-FU. At 25 and 200 μg/mL, the effectiveness of 2B co-crystals is significantly greater than that of API alone as

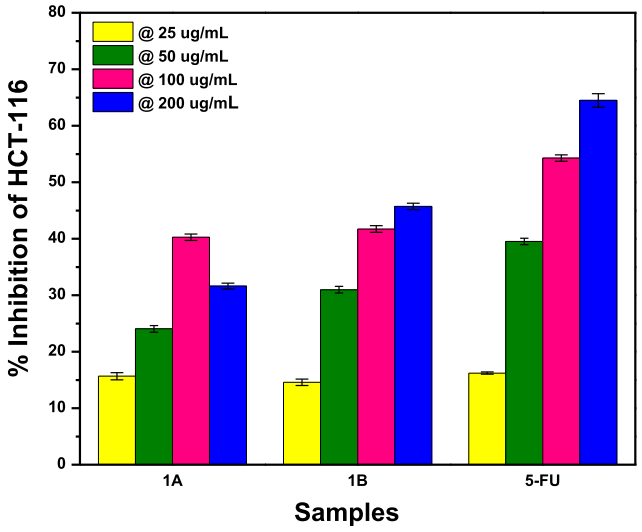

Fig. 9. Comparison of percentage growth inhibition of 5-FU-U co-crystals, fabricated by grinding (A) and solution (B) method, at varying concentrations of actinimycetes against HCT 116 colorectal cell lines.

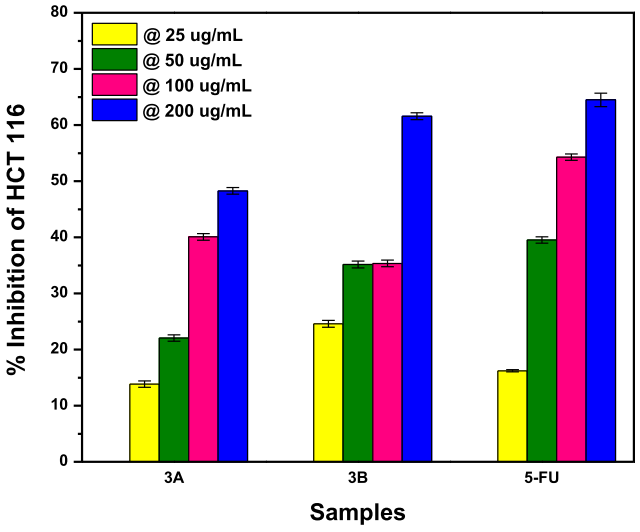

Fig. 11. Comparison of percentage growth inhibition of 5-FU-Ac co-crystals, fabricated by grinding (A) and solution (B) method, at varying concentrations of actinimycetes against HCT 116 colorectal cell lines.

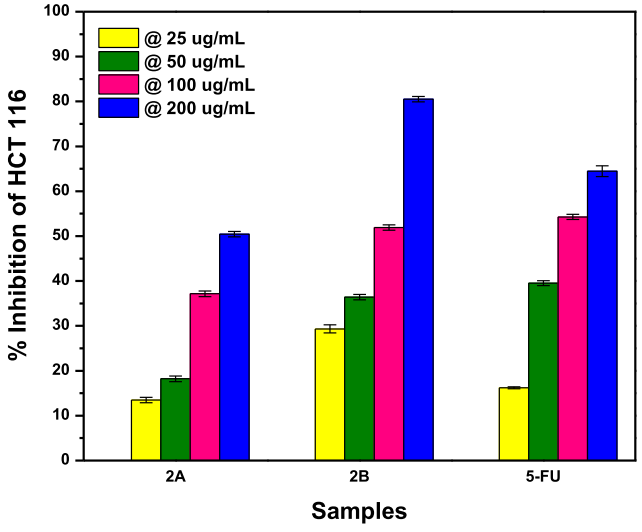

Fig. 10. Comparison of percentage growth inhibition of 5-FU-Th co-crystals, fabricated by grinding (A) and solution (B) method, at varying concentrations of actinimycetes against HCT 116 colorectal cell lines.

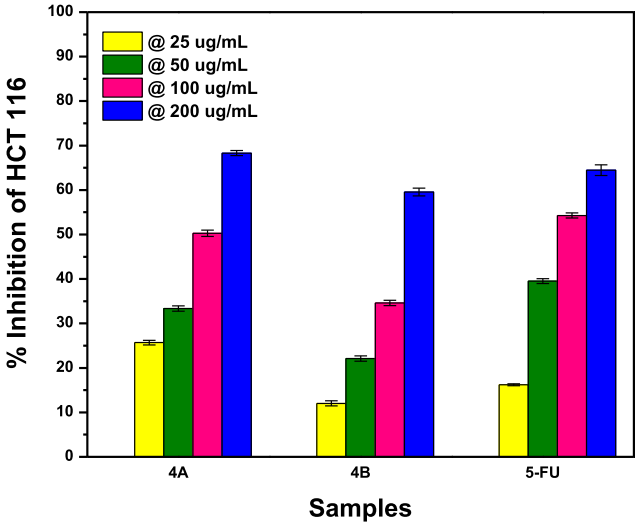

Fig. 12. Comparison of percentage growth inhibition of 5-FU-As co-crystals, fabricated by grinding (A) and solution (B) method, at varying concentrations of actinimycetes against HCT 116 colorectal cell lines.

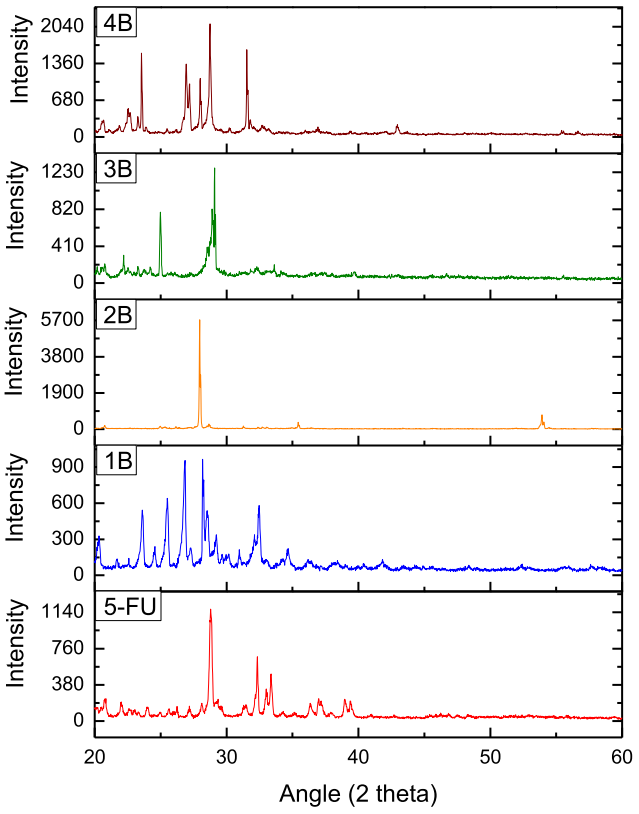

Fig. 13. Comparison of PXRD spectra of API and Co-formers fabricated by solution method (B).

shown in Fig. 10. This enhanced anticancer potential of 5-FU-Th co-crystals is attributed to an antioxidant potential of thiourea (Shakeel, 2016). It is clearly exhibited from Table 3, that the anticancer potential of 5-FU-Ac cocrystals followed the same trend as found for 5-FU-Th co-crystals i.e., Fig. 11 (3B) co-crystals are more effective anticancer agents than Fig. 11 (3A) except at 100 μg/mL. Now if the API and 3B co-crystals are compared, both have comparable anticancer potential at all the four concentrations possibly due to the larger molecule of acetanilide consequently weaker interactions with 5-FU leading to an easy release of API.

Both the cocrystals of 5-FU-As follow the general trend of increasing growth inhibition with increasing *actinomycetes* concentration however; this is the only co-former in this study whose Fig. 12 (4A), grinding method co-crystals exhibited greater anticancer potential than 4B (Solution method). Aspirin's own anticancer potential (Langley and Rothwell, 2012) made the 4A co-crystals almost as effective as API at all the concentrations of actinomycetes. The lesser effectiveness of 4B co-crystals can be justified by the stronger hydrogen bonding interactions of 4B co-crystals than 4A as evidenced from FTIR results leading to a slower release of API (Fig.12). If we consider the comparative response of all the co-crystals and API at individual concentrations, the following trends were observed in the order of decreasing effectiveness.

At 25 μg/mL, and 200 μg/mL**,** 5-FU-Th (Fig. 10) co-crystals obtained through solution method (2B) proved to be the co-crystals responsible for maximum growth inhibition as shown in Table 2 While at 50 μg/mL and 100 μg/mL API alone was the best suited growth inhibitor. Increasing *actinomycetes* (target) concentrations increased the subsequent growth inhibition. However, the rate of increase is different for all the co-formers due to the different nature of all the co-formers. The best outcomes of co-crystals like 5-FU-Th regarding MTT assay might be attributed to the readily release of the API and increased effectiveness as compared to 5-FU are supposed to be due to the individual pharmaceutical effectiveness of co-formers (Zhao, 2019).

As all the selected co-formers have their own proved pharmaceutical significance (Langley and Rothwell, 2012; Shakeel, 2016), so these changes in the activity of 5-FU after the formation of co-crystals very much rational and these trends might be attributed to the individual properties of all the co-formers. From the obtained results, it could be inferred that the solution method might be the favourable one for the maximum growth inhibition especially in the case of 5-FU-Th (2B) and 5-FU-Ac (3B) co-crystals, confirms from Figs. 10 and 11. To the best of our knowledge, MTT assays are not reported in any published study on 5-FU co-crystals. Nadzri and co-workers (Nadzri, 2016) reported anticancer activities of the synthesised co-crystals but the author focused on the binding affinities of co-crystals with targeted protein, not on the percent growth inhibition. In another study, Dai (2016), focused on the membrane permeability of synthesised

Table 2
Percentage inhibition of cancer cells HCT-116 using different concentrations.

Sample ID	%age Inhibition of cancer cells HCT-116 using different concentrations			
	25 μg/mL	50 μg/mL	100 μg/mL	200 μg/mL
5FU	16.21 ± 0.20	39.53 ± 0.56	54.28 ± 0.56	64.48 ± 1.21
1A	15.66 ± 0.64	24.04 ± 0.59	40.26 ± 0.58	31.60 ± 0.53
1B	14.57 ± 0.57	30.97 ± 0.58	41.71 ± 0.58	45.72 ± 0.57
2A	13.48 ± 0.59	18.21 ± 0.63	37.16 ± 0.63	50.46 ± 0.60
2B	29.33 ± 0.89	36.43 ± 0.60	51.91 ± 0.58	80.51 ± 0.59
3A	13.84 ± 0.57	22.04 ± 0.57	40.07 ± 0.59	48.27 ± 0.58
3B	24.59 ± 0.60	35.15 ± 0.62	35.3 ± 0.59	61.57 ± 0.60
4A	25.68 ± 0.54	33.35 ± 0.60	50.27 ± 0.59	68.31 ± 0.58
4B	12.02 ± 0.56	22.12 ± 0.60	34.61 ± 0.58	59.56 ± 0.88

Table 3
Crystallite Size of 5-FU and Co-crystals using Scherrer equation (Reinsch, 2016).

Sample ID	2θ	Intensity	Θ	θ in Radians	Cos θ	FWHM	Crystallite Size (Å)
5-FU	28.80°	1156	14.40	0.25	0.97	0.24	6.01
5-FU-U (1B)	28.19°	938	14.09	0.25	0.97	0.13	11.04
5-FU-Th (2B)	27.97°	5725	13.98	0.24	0.97	0.06	22.48
5-FU-Ac (3B)	29.10°	1249	14.55	0.25	0.97	0.051	27.85
5-FU-As (4B)	28.74°	2066	14.36	0.25	0.97	0.16	9.09

cocrystals. So, this is the first time in this study, MTT assays of synthesised co-crystals were performed and all the eight synthesised co-crystals proved to be effective from the obtained results.

In addition to the evidences of co-crystal formation through hydrogen bonding interactions and structural verification and its biological effectiveness with the help of their *in vitro* cytotoxic evaluation, it is important to add the significance and feasibility of the methodologies opted for the synthesis. The marvellous phenomenon of green chemistry was the aim behind the selection of both the protocols to carry out the synthesis in the environment friendly way with maximum output. The apparatus and chemicals used were easily available and economical. All the chemicals used were nonhazardous required in very low amount (Baumgartner, 2017). Further the selected co-formers were also not expensive. All the co-crystals developed at ambient temperature and pressure (Ahmed, 2016). The product gain in all the eight cases was maximum as there was no byproducts formation evidenced visually or through FTIR and PXRD analysis. As there was no byproduct formation, therefore, there was no stress to getting rid of waste byproducts at the end of the synthesis. In short, the whole synthesis process complies the rules of green chemistry devised by IUPAC (Reinsch, 2016).

4. Conclusions

Eight different co-crystals were prepared. All four co-formers were selected after a keen study on their pharmacological properties and subsequent metabolites. The successful co-crystals were formed at room temperature following both the methodologies, also supported by PXRD and FTIR results. Through both, the characterization techniques, significant shifts in the anticipated peaks of 5-FU were observed as the spectra of API and co-crystals were studied in comparison. In all the FTIR spectra of co-crystals, the main peaks of interest that are —N—H (3409.02 cm^{-1}) and —C=O (1647.77 cm^{-1}) were significantly shifted than the spectrum of 5-FU following the same trend reported in the literature. Through PXRD, the most intense characteristic peak of 5-FU is at 2θ = 28.79918°. This peak is not only shifted in position in all the graphs of co-crystals but also in intensity and FWHM values. Moreover, the appearance of new peaks in the graphs of co-crystals in comparison to API proved the formation of new molecules. 5-FU-Ac co-crystals and 5-FU-Th co-crystals obtained through solution method proved to be the co-crystals with the highest trend of preferred orientation and increased crystallinity. MTT assay proved that all the co-crystals manifested their activity against HCT 116 colorectal cell lines. Through anticancer results, again the 5-FU-Ac and 5-FU-Th co-crystals obtained through solution method proved to be the best agents for maximum growth inhibition, agreeing with the result of FTIR and PXRD. In short, this study is based on the very novel and the new phenomenon of co-crystallisation. Due to its simplicity, cost-effectiveness, easy fabrication protocols, no by-products formation and successful derivatization of API, this phenomenon may prove to be effective for future discoveries in cancer treatment. After the method optimization and estimation of anticancer potential of these co-crystals, the as prepared supramolecular synthons can be further bio-evaluated for the estimation of their *invivo* safety. Moreover; working in the same line many effective co-formers can also be studied for their contribution in the anticancer domain that is actually the need of the hour.

Appendix A. Supplementary material

Supplementary data to this article can be found online at https://doi.org/10.1016/j.jsps.2019.09.013.

References

Zhang, X. et al., 2018. Podophyllotoxin derivatives as an excellent anticancer aspirant for future chemotherapy: a key current imminent needs. Bioorg. Med. Chem. 26 (2), 340–355.

Zha, G.F. et al., 2019. Pharmaceutical significance of azepane based motifs for drug discovery: a critical review. Eur. J. Med. Chem. 162, 465–494.

Zhao, C. et al., 2018. Arylnaphthalene lactone analogues: synthesis and development as excellent biological candidates for future drug discovery. RSC Adv. 8 (17), 9487–9502.

Jubeen, F. et al., 2018. Eco-friendly synthesis of pyrimidines and its derivatives: a review on broad spectrum bioactive moiety with huge therapeutic profile. Synth. Commun. 48 (6), 601–625.

Rakesh, K.P. et al., 2017. Benzisoxazole: a privileged scaffold for medicinal chemistry. Med. Chem. Commun. 8, 2023–2039.

Moku, B. et al., 2019. The significance of N-methylpicolinamides in the development of anticancer therapeutics: synthesis and structure-activity relationship (SAR) studies. Bioorg. Chem. 86, 513–537.

Wang, M. et al., 2018. Amino acids/peptides conjugated heterocycles: a tool for the recent development of novel therapeutic agents. Bioorg. Chem. 76, 113–129.

Carrillo, E. et al., 2015. 5-Fluorouracil derivatives: a patent review (2012–2014). Exp. Opin. Ther. Pat. 25 (10), 1131–1144.

Qin, H.L. et al., 2016. Synthesis of alpha, beta-Unsaturated carbonyl-based compounds, oxime and oxime ether analogs as potential anticancer agents for overcoming cancer multidrug resistance by modulation of efflux pumps in tumor cells. J. Med. Chem. 59 (7), 3549–3561.

Qin, H.L. et al., 2017. Synthesis and mechanistic studies of curcumin analog-based oximes as potential anticancer agents. Chem. Biol. Drug Des. 90 (3), 443–449.

Zha, G.F. et al., 2017. Discovery of potential anticancer multi-targeted ligustrazine based cyclohexanone and oxime analogs overcoming the cancer multidrug resistance. Eur. J. Med. Chem. 135, 34–48.

Radwan, A.A., Alanazi, F.K., 2014. Design and synthesis of new cholesterol-conjugated 5-fluorouracil: a novel potential delivery system for cancer treatment. Molecules 19 (9), 13177–13187.

Miura, K. et al., 2010. 5-fu metabolism in cancer and orally-administrable 5-fu drugs. Cancers 2 (3), 1717–1730.

Zhang, Q. et al., 2018. New utilization of Polygonum multiflorum polysaccharide as macromolecular carrier of 5-fluorouracil for controlled release and immunoprotection. Int. J. Biol. Macromol. 116, 1310–1316.

Petaccia, M. et al., 2016. Correction: Inclusion of new 5-fluorouracil amphiphilic derivatives in liposome formulation for cancer treatment. MedChemComm 7 (2). 378-378.

Köksal Karayildirim, Ç. et al., 2018. Formulation, characterization, cytotoxicity and Salmonella/microsome mutagenicity (Ames) studies of a novel 5-fluorouracil derivative. Saudi Pharmaceut. J.: SPJ: Off. Publicat. Saudi Pharmaceut. Soc. 26 (3), 369–374.

Ofonime Udofot, K.A., Israel, Bridg'ette, Agyare, Edward, 2015. Cytotoxicity of 5-fluorouracil-loaded pH-sensitive liposomal nanoparticles in colorectal cancer cell lines. Integr. Cancer Sci Ther 2 (5), 245–252.

Zhou, G. et al., 2013. Aspirin hydrolysis in plasma is a variable function of butyrylcholinesterase and platelet-activating factor acetylhydrolase 1b2 (PAFAH1b2). J. Biol. Chem. 288 (17), 11940–11948.

Tummala, S., Kumar, MNS., Prakash, 2015. A Formulation and characterization of 5-Fluorouracil enteric coated nanoparticles for sustained and localized release in treating colorectal cancer. Saudi Pharmaceut. J., vol. 23, 3, pp. 308–314.

Subudhi, M.B. et al., 2015. Eudragit S100 coated citrus pectin nanoparticles for colon targeting of 5-fluorouracil. Materials 8 (3), 832–849.

Dong, P. et al., 2019. Innovative nano-carriers in anticancer drug delivery-a comprehensive review. Bioorg. Chem. 85, 325–336.

Stoler, E., Warner, J., 2015. Non-covalent derivatives: cocrystals and eutectics. Molecules 20 (8), 14833–14848.

Nadzri, N.I. et al., 2016. 5-fluorouracil co-crystals and their potential anti-cancer activities calculated by molecular docking studies. J. Chem. Crystallogr. 46 (3), 144–154.

Douroumis, D., Ross, S.A., Nokhodchi, A., 2017. Advanced methodologies for cocrystal synthesis. Adv. Drug Deliv. Rev. 117, 178–195.

Karimi-Jafari, M. et al., 2018. Creating cocrystals: a review of pharmaceutical cocrystal preparation routes and applications. Cryst. Growth Des. 18 (10), 6370–6387.

Likhitha, U. et al., 2019. Do hydrogen bonding and noncovalent interactions stabilize nicotinamide-picric acid cocrystal supramolecular assembly?. J. Mol. Struct. 1195, 827–838.

Delori, A., Eddleston, M.D., Jones, W., 2013. Cocrystals of 5-fluorouracil. CrystEngComm 15 (1), 73–77.

Mohana, M., Muthiah, P.T., McMillen, C.D., 2017. Supramolecular hydrogen-bonding patterns in 1:1 cocrystals of 5-fluorouracil with 4-methylbenzoic acid and 3-nitrobenzoic acid. Acta Crystallogr. C Struct. Chem. 73 (Pt 3), 259–263.

Dai, X.-L. et al., 2016. Improving the membrane permeability of 5-fluorouracil via cocrystallization. Cryst. Growth Des. 16 (8), 4430–4438.

Langley, R.E., Rothwell, P.M., 2012. Potential biomarker for aspirin use in colorectal cancer therapy. Nat. Rev. Clin. Oncol. 10, 8.

Li, J.P. et al., 2017. Quantitative determination of five metabolites of aspirin by UHPLC-MS/MS coupled with enzymatic reaction and its application to evaluate the effects of aspirin dosage on the metabolic profile. J. Pharm. Biomed. Anal. 138, 109–117.

Rakesh, K.P. et al., 2017. Synthesis and SAR studies of potent H+/K+-ATPase and anti-inflammatory activities of symmetrical and unsymmetrical urea analogues. Med. Chem. Res. 26 (8), 1675–1681.
Fang, W.Y. et al., 2019. Synthetic approaches and pharmaceutical applications of chloro-containing molecules for drug discovery: a critical review. Eur. J. Med. Chem. 173, 117–153.
Ahmed, S. et al., 2016. A review on plants extract mediated synthesis of silver nanoparticles for antimicrobial applications: a green expertise. J. Adv. Res. 7 (1), 17–28.
Ansari, M.D. et al., 2019. Organo-nanocatalysis: an emergent green methodology for construction of bioactive oxazines and thiazines under ultrasonic irradiation. J. Mol. Struct. 1196, 54–57.
Suthindhiran, K., Kannabiran, K., 2009. Cytotoxic and antimicrobial potential of actinomycete species Saccharopolyspora salina VITSDK4 Isolated from the Bay of Bengal Coast of India. Am. J. Infect. Diseases 5 (2), 90–98.
Sonawane, R.P., 2014. Green synthesis of pyrimidine derivative. Int. Lett. Chem., Phys. Astron. 2, 64–68.
Moisescu-Goia, C., Muresan-Pop, M., Simon, V., 2017. New solid state forms of antineoplastic 5-fluorouracil with anthelmintic piperazine. J. Mol. Struct. 1150, 37–43.
Yan, X. et al., 2009. Synthesis and structure–antitumor activity relationship of sulfonyl 5-fluorouracil derivatives. Phos., Sulfur, Silicon 185 (1), 158–164.
Li, S., Chen, J.-M., Lu, T.-B., 2014. Synthon polymorphs of 1: 1 co-crystal of 5-fluorouracil and 4-hydroxybenzoic acid: their relative stability and solvent polarity dependence of grinding outcomes. CrystEngComm 16 (28), 6450–6458.
Fang, F.-Q. et al., 2015. Anti-cancer effects of 2-oxoquinoline derivatives on the HCT116 and LoVo human colon cancer cell lines. Mol. Med. Rep. 12 (6), 8062–8070.
Qin, H.-L. et al., 2015. Molecular docking studies and biological evaluation of chalcone based pyrazolines as tyrosinase inhibitors and potential anticancer agents. RSC Adv. 5 (57), 46330–46338.
Vichai, V., Kirtikara, K., 2006. Sulforhodamine B colorimetric assay for cytotoxicity screening. Nat. Protoc. 1 (3), 1112–1116.
Patel, S. et al., 2009. In-vitro cytotoxicity activity of Solanum nigrum extract against Hela cell line and Vero cell line. Int. J. Pharm. Pharm. Sci. 1 (1), 38–46.
Abdelghani, E. et al., 2017. Synthesis and antimicrobial evaluation of some new pyrimidines and condensed pyrimidines. Arab.J. Chem. 10, S2926–S2933.
Shakeel, A., 2016. Thiourea derivatives in drug design and medicinal chemistry: a short review. J. Drug Des. Med. Chem. 2 (1), 10.
Zhao, C. et al., 2019. Pharmaceutical and medicinal significance of sulfur (S(VI))-Containing motifs for drug discovery: a critical review. Eur. J. Med. Chem. 162, 679–734.
Baumgartner, B. et al., 2017. Green and highly efficient synthesis of perylene and naphthalene bisimides in nothing but water. Chem. Commun. (Camb.) 53 (7), 1229–1232.
Reinsch, H., 2016. "Green" synthesis of metal-organic frameworks. Eur. J. Inorg. Chem. 2016 (27), 4290–4299.